

- [20] A full account of the calculations with structures and energies for all of the examined cases, that is, the search of conformational space, is in preparation. Cartesian coordinates and energies for validation for all structures reported herein are given in the Supporting Information.
- [21] O. M. Aagaard, R. J. Meier, F. Buda, *J. Am. Chem. Soc.* **1998**, *120*, 7174; R. J. Meier, O. M. Aagaard, F. Buda, *J. Mol. Catal. A* **2000**, *160*, 189; S. F. Vyboshchikov, M. Bühl, W. Thiel, *Chem. Eur. J.* **2002**, *8*, 3962.
- [22] C. A. Tolman, *Chem. Rev.* **1977**, *77*, 313.
- [23] J. W. Faller, B. V. Johnson, *J. Organomet. Chem.* **1975**, *96*, 99; W. D. Jones, F. J. Feher, *Inorg. Chem.* **1984**, *23*, 2376; J. Polowin, M. C. Baird, *J. Organomet. Chem.* **1994**, *478*, 45; F. P. Fanizzi, M. Lanfranchi, G. Natile, A. Tiripicchio, *Inorg. Chem.* **1994**, *33*, 3331; J. Albert, R. Bosque, J. M. Cadena, S. Delgado, J. Granell, *J. Organomet. Chem.* **2001**, *634*, 83.
- [24] B. Breit, R. Winde, T. Mackewitz, R. Paciello, K. Harms, *Chem. Eur. J.* **2001**, *7*, 3106; B. Breit, *J. Mol. Catal. A* **1999**, *143*, 143; B. Breit, R. Winde, K. Harms, *J. Chem. Soc. Perkin Trans. 1* **1997**, 2681.

Solvothermal Synthesis, Crystal Structure, Thermal Stability, and Mössbauer Spectroscopic Investigation of the Mixed-Valent Thioantimonate(III,V) $[\text{Ni}(\text{dien})_2]_2\text{Sb}_4\text{S}_9$ **

Ralph Stähler, Bernd-Dieter Mosel, Hellmut Eckert, and Wolfgang Bensch*

During the last decade it was impressively demonstrated by several groups that the solvothermal technique is not only a promising route for the preparation of new and exciting open framework oxidic compounds but also for the syntheses of fascinating thio- and selenometalates.^[1–7] Since the pioneering work of Schäfer and co-workers,^[8] about 50 new thioantimonates have been prepared and characterized. In most compounds antimony occurs as Sb^{III} and, because of the variable coordination behavior caused by the stereochemically active lone pair,^[9] the dimensionalities of the anionic Sb_xS_y frameworks range over 1D chains, 2D layers, and 3D interconnection of the SbS_3 primary building units. Thioantimonates(V) always contain tetrahedral $[\text{Sb}^{\text{V}}\text{S}_4]^{3-}$ ions that are not further interconnected or condensed. To date the coexistence of Sb^{III} and Sb^{V} within a polymeric thioantimonate anion was never observed.

Normally solvothermal syntheses are performed using organic molecules as structure-directors. Recently, we demonstrated that transition-metal complexes can also be used as

“template” molecules^[11–13,15–18]. During our systematic experiments with the in situ formed $[\text{Ni}(\text{dien})_2]^{2+}$ ion (dien = diethylenetriamine) as the structure-directing molecule, we synthesized and fully characterized the first mixed-valent thioantimonate anion $[\text{Sb}_4\text{S}_9]^{4-}$ which contains Sb^{III} and Sb^{V} . The title compound was obtained under solvothermal conditions as yellow polyhedra that are stable to air, in water, and in acetone. The results of a large number of syntheses performed at different temperatures and for different reaction times suggest that the $[\text{Ni}(\text{dien})_2]_2\text{Sb}_4\text{S}_9$ is formed at higher temperatures and in short reaction times. The compound crystallizes in the monoclinic space group $P2_1/c$.^[10]

The $[\text{Sb}_4\text{S}_9]^{4-}$ ion is composed of three $\text{Sb}^{\text{III}}\text{S}_3$ pyramids (Sb2 , Sb3 , and Sb4), which share common corners leading to the formation of an Sb_3S_7 moiety (Figure 1). The Sb1 atom is in a tetrahedral coordination environment of four S atoms to form a $\text{Sb}^{\text{V}}\text{S}_4$ tetrahedron. The interconnection of the Sb_3S_7 unit and the $\text{Sb}^{\text{V}}\text{S}_4$ tetrahedron through the S4 atom yields the $[\text{Sb}_4\text{S}_9]^{4-}$ ionic chain. The bond lengths in the $\text{Sb}^{\text{III}}\text{S}_3$ units are between 2.331(1) and 2.637(1) Å, with S– Sb^{III} –S angles ranging from 88.33(3) to 102.21(4)°. The longest Sb–S bond is between Sb2 and S4 joining the Sb_3S_7 and SbS_4 units.

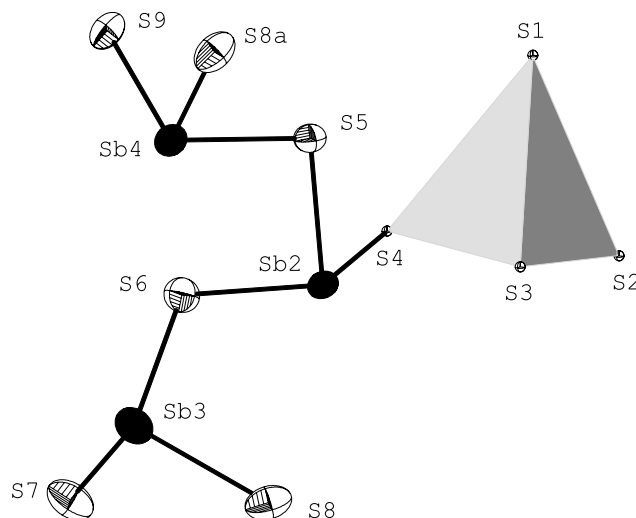


Figure 1. The $[\text{Sb}_4\text{S}_9]^{4-}$ ion with labelling. The $\text{Sb}^{\text{V}}\text{S}_4$ unit is shown as a tetrahedron. The displacement ellipsoids are drawn at the 50 % probability level. Selected bonds angles [°]: S1–Sb1–S2 113.64(4), S1–Sb1–S3 110.33(4), S1–Sb1–S4 110.36(4), S2–Sb1–S3 109.86(4), S2–Sb1–S4 106.02(4), S3–Sb1–S4 106.30(4). Symmetry code for S8a: $-x, -0.5 + y, 0.5 - z$.

The Sb^{III} –S interatomic distances, as well as the angles, are in the range reported in the literature.^[2,5,7,11–15] The $\text{Sb}^{\text{V}}\text{S}_4$ interatomic distances are significantly shorter than Sb^{III} –S bonds and vary between 2.294(1) and 2.390(1) Å, with S–Sb1–S angles ranging from 106.02(4) to 113.64(4)°, which indicate only a slight deviation from the ideal tetrahedral geometry. $\text{Sb}^{\text{V}}\text{S}_4$ interatomic distances and S– Sb^{V} –S angles are in the range found in the literature.^[12,16,17] The anionic chains have a sinusoidal shape and run along [010] (Figure 2). The $\text{Sb}^{\text{V}}\text{S}_4$ tetrahedra are located at the exterior of the central Sb_3S_7 backbone of the anion. The compound decomposes in two steps starting at about $T_{\text{onset}} = 257^\circ\text{C}$, as evidenced by differential thermal analysis–thermogravimetric analysis–

[*] Prof. Dr. W. Bensch, Dipl.-Chem. R. Stähler
Institut für Anorganische Chemie
Universität Kiel
Olshausenstrasse 40, 24098 Kiel (Germany)
Fax: (+49)431–880–1520
E-mail: wbensch@ac.uni-kiel.de
Dr. B.-D. Mosel, Prof. Dr. H. Eckert
Institut für Physikalische Chemie
Westfälische Wilhelms-Universität Münster
Schlossplatz 7, 48149 Münster (Germany)

[**] This work was supported by the States of Schleswig-Holstein and Nordrhein-Westfalen, and the Fonds der Chemischen Industrie. dien = diethylenetriamine.

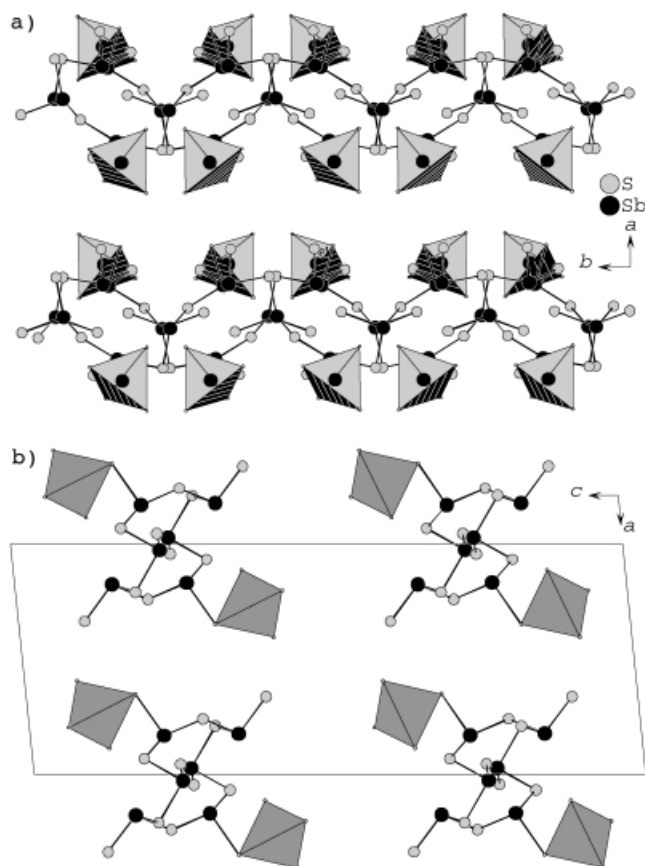


Figure 2. Arrangement of the anion in $[\text{Ni}(\text{dien})_2]_2\text{Sb}_4\text{S}_9$ with a view along $[001]$ (a) and $[010]$ (b).

mass spectrometry (DTA–TG–MS) experiments. The degradation is accompanied by two weight losses ($-\Delta m_{\text{exp}1} = 30.5\%$ and $-\Delta m_{\text{exp}2} = 3.5\%$) and by one strong endothermic peak in the curve at $T_p = 270.8^\circ\text{C}$ with a shoulder at $T_p = 277^\circ\text{C}$, and one small broad endothermic signal at $T_p = 328^\circ\text{C}$. The experimental mass change corresponds roughly with the loss of the dien ligands in the first step ($-\Delta m_{\text{theo}(\text{dien})} = 31.6\%$) and the emission of H_2S in the second step ($-\Delta m_{\text{theo}(\text{H}_2\text{S})} = 2.6\%$, $m/z_{\text{H}_2\text{S}} = 34$). The shoulder in the spectrum at $T_p = 277^\circ\text{C}$ was often observed during the thermal decomposition of compounds containing $[\text{M}(\text{dien})_2]^{2+}$ ($\text{M} = \text{Fe}, \text{Ni}$) complexes.^[11,12,15] In the gray decomposition product Sb_2S_3 , NiS , and NiSbS were identified by X-ray powder diffraction.

The mixed-valence character of $[\text{Ni}(\text{dien})_2]_2\text{Sb}_4\text{S}_9$ is unambiguously demonstrated by the ^{121}Sb Mössbauer spectrum shown in Figure 3, which also includes the spectra of some suitable reference compounds. The lineshape parameters obtained by least-squares fitting are listed in Table 1. Clearly, the spectrum of $[\text{Ni}(\text{dien})_2]_2\text{Sb}_4\text{S}_9$ is a superposition of two lineshape contributions. The contribution centered near -12.5 mm s^{-1} reflects all the typical lineshape parameters of Sb^{III} compounds.^[19] The lineshape is asymmetrically broadened by the effect of strong nuclear electric quadrupolar interactions. These interactions reflect a large electric field gradient, created at the ^{121}Sb site by the local ligand distribution and the partially hybridized electron pair. The contribution near -5.7 mm s^{-1} is attributable to the Sb^{V} site. For this species, no quadrupolar interactions are detectable,

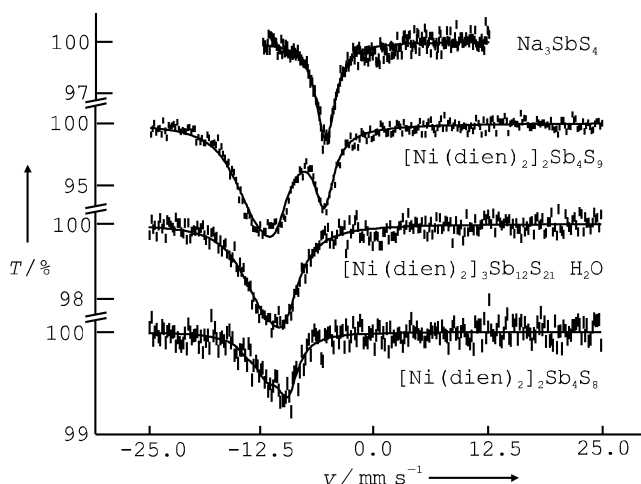


Figure 3. ^{121}Sb Mössbauer spectra of thioantimonates. From top to bottom: Na_3SbS_4 (4.2 K), $[\text{Ni}(\text{dien})_2]_2\text{Sb}_4\text{S}_9$ (4.2 K), $[\text{Ni}(\text{dien})_2]_3\text{Sb}_{12}\text{S}_{21} \cdot \text{H}_2\text{O}$ (78 K), and $[\text{Ni}(\text{dien})_2]_2\text{Sb}_4\text{S}_8$ (78 K).

Table 1. ^{121}Sb Mössbauer isomer shifts (IS), quadrupolar splittings (QS), and linewidths (Γ) of the thioantimonate compounds of the present study. All values are given in mm s^{-1} .

Compound	IS (± 0.2)	QS (± 0.4)	Γ (± 0.2)	Oxidation state
Na_3SbS_4	−5.5	0.0	2.6	Sb^{V}
$[\text{Ni}(\text{dien})_2]_2\text{Sb}_4\text{S}_9$	−5.7	0.0	2.6	Sb^{V}
	−12.5	−14.3	3.8	Sb^{III}
$[\text{Ni}(\text{dien})_2]_2\text{Sb}_4\text{S}_8$	−11.0	−15.9	2.7	Sb^{III}
$[\text{Ni}(\text{dien})_2]_3\text{Sb}_{12}\text{S}_{21} \cdot \text{H}_2\text{O}$	−11.4	−14.8	4.0	Sb^{III}

which suggests a highly symmetric local environment, as is typically observed for pentavalent antimony in solids. The area ratio determined from the transmission integral fit is 76.8:23.2, which is in close agreement with the value (3:1) expected from the crystallographically determined structure. This result also confirms that at 4.2 K the Lamb–Mössbauer factors for both antimony species are very similar.

Experimental Section

Yellow polyhedra of $[\text{Ni}(\text{dien})_2]_2\text{Sb}_4\text{S}_9$ were obtained by treating a mixture of elemental Ni (0.058 g, 1 mmol), Sb (0.121 g, 1 mmol), and S (0.096 g, 3 mmol) in a 50% water solution of dien (2 mL) under solvothermal conditions. The slurry was heated in an autoclave to 140°C , held at this temperature for ten days and cooled to room temperature within 3 h. The products were filtered off, washed with water and acetone, and dried under vacuum. The yield was 10% based on Ni. The main product (55%) was identified as $[\text{Ni}(\text{dien})_2]_3(\text{SbS}_4)_2$ ^[12] and is stable to air, in water, and in acetone. Stirring the reaction mixture during the synthesis, increasing the temperature to $180\text{--}200^\circ\text{C}$, and reducing the reaction time to about 1.5 h resulted in a phase-pure product (45% based on Ni). Elemental analysis (%) calcd: C 14.72, H 4.01, N 12.87, S 22.10; found: C 13.43, H 3.61, N 10.97, S 21.39.

DTA–TG–MS measurements were performed on a STA-409CD device from Netzsch. All measurements were corrected for buoyancy and current effects, and were made with a heating rate of 4 K min^{-1} in Al_2O_3 crucibles under a dynamic helium atmosphere (flow rate: 75 mL min^{-1} , purity: 5.0). 37.2 keV Mössbauer spectra were obtained in transmission geometry using a $\text{Ba}^{121\text{m}}\text{SnO}_3$ source (activity 18 MBq) from New England Nuclear. The samples were investigated within polyacrylate containers of 3 cm^2 area; typically 100–200 mg of sample was used. Sample thicknesses were adjusted to 10 mg Sb cm^{-2} . To maximize the Lamb–Mössbauer factors the samples

were measured at low temperatures (4.2 K or 78 K). The source was kept at room temperature. Spectra were recorded over a velocity range of $\pm 25 \text{ mms}^{-1}$ using an NaI(Tl) scintillation counter. Fitting of the spectra was carried out on the basis of the theoretically expected lineshape arising from the allowed transitions between the quadrupolar-split energy levels of the ground state ($I = 5/2$) and the excited state ($I = 7/2$).

Received: June 27, 2002 [Z19623]

Efficient Solid-Phase Synthesis of a Complex, Branched N-Glycan Hexasaccharide: Use of a Novel Linker and Temporary-Protecting-Group Pattern**

Xiangyang Wu, Matthias Grathwohl, and Richard R. Schmidt*

- [1] W. S. Sheldrick, M. Wachhold, *Coord. Chem. Rev.* **1998**, *176*, 211–322.
- [2] A. V. Powell, R. Paniagua, P. Vaqueiro, A. M. Chippindale, *Chem. Mater.* **2002**, *14*, 1220–1224.
- [3] W. S. Sheldrick, M. Wachhold, *Angew. Chem.* **1997**, *109*, 214–234; *Angew. Chem. Int. Ed.* **1997**, *36*, 206–224.
- [4] X. Wang, F. Liebau, *Acta Crystallogr. Sect. B.* **1996**, *52*, 7–15.
- [5] W. S. Sheldrick, H.-J. Häusler, *Z. Anorg. Allg. Chem.* **1988**, *557*, 105–111.
- [6] X. Wang, F. Liebau, *Z. Kristallogr.* **1996**, *211*, 437–439.
- [7] A. V. Powell, S. Boissiere, A. M. Chippindale, *J. Chem. Soc. Dalton Trans.* **2000**, *22*, 4192–4195.
- [8] a) G. Dittmar, H. Schäfer, *Z. Anorg. Allg. Chem.* **1977**, *437*, 183–187; b) G. Dittmar, H. Schäfer, *Z. Anorg. Allg. Chem.* **1975**, *414*, 211–219; c) G. Dittmar, H. Schäfer, *Z. Anorg. Allg. Chem.* **1978**, *441*, 93–97; d) G. Dittmar, H. Schäfer, *Z. Anorg. Allg. Chem.* **1978**, *441*, 98–102; e) B. Eisenmann, H. Schäfer, *Z. Naturforsch. B* **1979**, *34*, 383–385; f) G. Cordier, H. Schäfer, C. Schwidetzky, *Z. Naturforsch. B* **1984**, *39*, 131–134; g) K. Volk, P. Bickert, R. Kolmer, H. Schäfer, *Z. Naturforsch. B* **1979**, *34*, 380–382; h) G. Cordier, H. Schäfer, *Rev. Chim. Miner.* **1981**, *18*, 218–223; i) G. Cordier, H. Schäfer, C. Schwidetzky, *Rev. Chim. Miner.* **1985**, *22*, 722–727; j) H. A. Graf, H. Schäfer, *Z. Naturforsch. B* **1972**, *27*, 735–739.
- [9] X. Wang, F. Liebau, *Acta Crystallogr. Sect. B.* **1996**, *52*, 7–15.
- [10] a) The compound crystallizes in the monoclinic space group $P2_1/c$, $a = 11.743(2)$, $b = 11.358(2)$, $c = 30.878(6)$ Å, $\beta = 95.78(3)^\circ$, $V = 4097.5(14)$ Å³, $Z = 4$, $\rho = 2.117 \text{ mgm}^{-3}$, $\mu(\text{MoK}\alpha) = 3.99 \text{ mm}^{-1}$, $F(000) = 2544$. STOE AED-II diffractometer, monochromated $\text{MoK}\alpha$ radiation ($\lambda = 0.71073$ Å). Lorentz, polarization, and absorption corrections; 17068 reflections; range $1.74 \leq \theta \leq 27.53$; 9436 unique data; 8164 with $I \geq 2\sigma(I)$. Structure solution was performed with SHELXS-97 using direct methods.^[10b] Refinement was done against F^2 using SHELXL-97.^[10c] All heavy atoms were refined anisotropically. Several C atoms are disordered with occupancies given in parentheses: C6 (50%), C6' (50%), C9 (60%), C9' (40%), C11 (50%), C11' (50%), C13 (70%), C13' (30%). The hydrogen atoms were positioned with idealized geometry and refined with fixed isotropic displacement parameters using a riding model. Final reliability values: $R1 = 0.0344$ for all reflections, $wR2 = 0.0682$ for all reflections, goodness-of-fit = 1.058. CCDC-188070 contains the supplementary crystallographic data for this paper. These data can be obtained free of charge via www.ccdc.cam.ac.uk/conts/retrieving.html (or from the Cambridge Crystallographic Data Centre, 12 Union Road, Cambridge CB2 1EZ, UK; fax: (+44) 1223-336-033; or deposit@ccdc.cam.ac.uk); b) G. M. Sheldrick, SHELXS-97, Program for the Solution of Crystal Structures, Universität of Göttingen, Göttingen (Germany), 1997; c) G. M. Sheldrick, SHELXL-97, Program for the Refinement of Crystal Structures, University of Göttingen, Göttingen (Germany), 1997.
- [11] W. Bensch, C. Näther, R. Stähler, *Chem. Commun.* **2001**, *5*, 477–478.
- [12] R. Stähler, C. Näther, W. Bensch, *Acta Crystallogr. Sect. C* **2001**, *57*, 26–27.
- [13] R. Stähler, W. Bensch, *Z. Anorg. Allg. Chem.* **2002**, *628*, 1657–1662.
- [14] J. Ellermeier, W. Bensch, *Monatsh. Chem.* **2001**, *132*, 565–573.
- [15] R. Stähler, C. Näther, W. Bensch, *Eur. J. Inorg. Chem.* **2001**, 1835–1840.
- [16] M. Schur, W. Bensch, *Acta Crystallogr. Sect. C* **2000**, *56*, 1107–1108.
- [17] M. Schur, H. Rijnberk, C. Näther, W. Bensch, *Polyhedron* **1998**, *18*, 101–107.
- [18] R. Stähler, C. Näther, W. Bensch, unpublished work.
- [19] J. G. Stevens in “*Chemical Mössbauer Spectroscopy*”, (Ed.: R. H. Herber) Plenum Press, New York, **1984**, p. 319.

Oligosaccharides are known to be important molecules in various biological processes; therefore, they have gained increasing interest in recent years.^[1] However, in contrast to oligopeptides^[2] and oligonucleotides^[3] which are routinely constructed on automated synthesizers employing standardized building blocks and polymer supports, no generally applied synthetic methodology has yet appeared for the solid-phase synthesis of complex oligosaccharides.^[4] Success in this challenging task would provide several advantages over solution-phase techniques: 1) the required standardized building blocks could become commercially available, 2) an excess of building blocks and/or reagents could be used to drive reactions to completion, 3) the synthesis could become much faster, and 4) purification procedures could become simpler.

Another fundamental key issue for solid-phase oligosaccharide synthesis is the availability of a high-yielding and stereoselective glycosylation strategy. Of the various glycosyl donors employed for this purpose,^[5–11] *O*-glycosyl trichloroacetimidates^[12] are suitable because of their high glycosyl-donor properties in the presence of just catalytic amounts of a (Lewis) acid. In combination with solvent and temperature effects, type of catalyst, protecting-group pattern, and anchimeric assistance these donors also permit the desired control of the stereoselectivity at the anomeric center.^[13]

An additional requirement for solid-phase oligosaccharide synthesis is access to branching which is found in many oligosaccharides and glycoconjugates but not in peptides and oligonucleotides. Thus, for chain extension and branching, besides permanently protected functional groups, to be liberated only after completion of the solid-phase oligosaccharide synthesis, a suitable temporary-protecting-group pattern is required. This temporary-protecting-group pattern provides the orthogonality required for branching and should also accommodate the demands of the linker which necessitates an additional temporary functional group.

Based on our recent studies on new temporary protecting groups,^[12,14] new linker types,^[14] and the synthesis of branched oligosaccharides,^[12e,15] we report herein a novel strategy which

[*] R. R. Schmidt, Dipl.-chem. X. Wu, Dr. M. Grathwohl
Department of Chemistry
University of Konstanz
78457 Konstanz (Germany)
Fax: (+49) 7531-88-3135
E-mail: richard.schmidt@uni-konstanz.de

[**] This work was supported by the Deutsche Forschungsgemeinschaft, the Fonds der Chemischen Industrie, and the European Community (Grant No. HRPN-CT-2000-00001/GLYCOTRAIN).